Journal of Power Sources 244 (2013) 389–394

Contents lists available at SciVerse ScienceDirect

Journal of Power Sources

journal homepage: www.elsevier.com/locate/jpowsour

Direct ultraviolet-assisted conformal coating of nanometer-thick poly(tris(2-(acryloyloxy)ethyl) phosphate) gel polymer electrolytes on high-voltage $LiNi_{1/3}Co_{1/3}Mn_{1/3}O_2$ cathodes

Eun-Ho Lee [a], Jang-Hoon Park [a], Ju-Hyun Cho [a], Sung-Ju Cho [a], Dong Wook Kim [b], He Dan [b], Yongku Kang [b,**], Sang-Young Lee [c,*]

[a] Department of Chemical Engineering, Kangwon National University, Chuncheon, Kangwondo 200-701, Republic of Korea
[b] Advanced Battery Material Research Group, Division of Advanced Materials, Korea Research Institute of Chemical Technology, Daejeon 305-600, Republic of Korea
[c] Interdisciplinary School of Green Energy, Ulsan National Institute of Science and Technology (UNIST), Ulsan 689-798, Republic of Korea

HIGHLIGHTS

- Surface modification of high-voltage NCM cathode with PTAEP gel polymer electrolyte.
- Direct UV-assisted, conformal coating of PTAEP layers on as-formed NCM cathode.
- PTAEP nanocoating layers do not impair preformed structure of NCM cathode.
- PTAEP-NCM cathode shows superior cycling performance and thermal stability.
- Conformal PTAEP coating layers act as a new ion-conductive protective film.

GRAPHICAL ABSTRACT

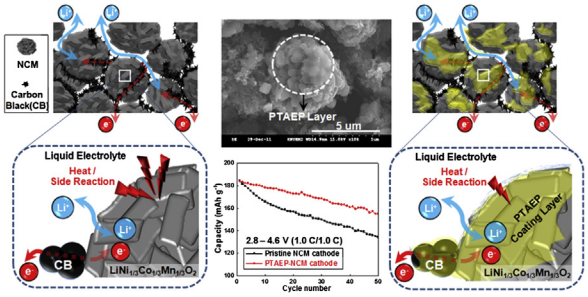

ARTICLE INFO

Article history:
Received 20 October 2012
Received in revised form
25 November 2012
Accepted 11 December 2012
Available online 20 December 2012

Keywords:
Lithium-ion batteries
High-voltage cathodes
Surface modification
Ultraviolet-assisted conformal coating
Poly(tris(2-(acryloyloxy)ethyl) phosphate)
Ion-conductive protective layers

ABSTRACT

As a facile and scalable approach to the surface modification of high-voltage cathode materials for lithium-ion batteries, direct UV-assisted conformal coating of poly(tris(2-(acryloyloxy)ethyl) phosphate) (PTAEP) gel polymer electrolyte on as-formed $LiNi_{1/3}Co_{1/3}Mn_{1/3}O_2$ (NCM) cathode is presented. The smooth and continuous PTAEP coating layer with nanometer-thickness (~20 nm) is successfully introduced on the NCM surface without impairing electronic/ionic conduction pathways preformed in the NCM cathode. Owing to this structural uniqueness, the PTAEP-coated NCM cathode significantly improves the high-voltage (4.6 V) cycling performance and mitigates the exothermic reaction between the delithiated NCM and liquid electrolyte. This demonstrates that the conformal PTAEP nanocoating layer proposed herein, which is completely different from conventional inorganic material-based coating layers, acts as a new ion-conductive protective film that effectively suppresses unwanted interfacial side reactions between the high-voltage cathode materials and liquid electrolyte.

© 2012 Elsevier B.V. All rights reserved.

1. Introduction

As lithium-ion batteries vigorously expand into newly emerging application fields such as smart mobile devices, power

* Corresponding author. Tel.: +82 52 217 2948; fax: +82 52 217 2019.
** Corresponding author. Tel.: +82 42 860 7207; fax: +82 42 860 7200.
E-mail addresses: ykang@krict.re.kr (Y. Kang), syleek@unist.ac.kr (S.-Y. Lee).

0378-7753/$ – see front matter © 2012 Elsevier B.V. All rights reserved.
http://dx.doi.org/10.1016/j.jpowsour.2012.12.049

tools, (hybrid) electric vehicles, and energy storage systems, the demand for high-energy density/high-power density cells is rapidly growing [1–5]. Among various attempts to meet this stringent requirement, charging cells at a voltage higher than the conventional cut-off at 4.2 V has been suggested as one of the most secured approaches to enhance the energy/power density of cells [6–10]. Raising the charge cut-off voltage, however, tends to face formidable challenges related to deterioration of cell performance and thermal stability of cathode materials. This is mainly due to undesirable interfacial side reactions between delithiated cathode materials and liquid electrolytes, wherein liquid electrolytes are highly vulnerable to electrochemical decomposition particularly at high-voltage conditions. Hence, it should be noted that the understanding and control of interfacial phenomena between the cathode materials and liquid electrolytes are needed for facilitating the successful development of high-voltage cells.

One promising approach to resolve these stringent shortcomings of high-voltage cathode materials is the surface modification using inorganic coating materials such as Al_2O_3 [11,12], ZrO_2 [13], ZnO [14], AlF_3 [15], $Ni_3(PO_4)_2$ [16], and $AlPO_4$ [17]. Unfortunately, these inorganic materials tend to be discontinuously deposited on cathode material surface and also behave as a resistive layer impeding ionic and electronic transport, although they do suppress the interfacial side reactions between cathode materials and liquid electrolytes. Moreover, the inorganic coatings often require complex and cost-consuming processing steps.

Meanwhile, on the basis of film-forming capability and ionic conductivity of coating layers, gel polymer electrolytes (GPEs) can be proposed as an effective coating material [18,19]. Herein, motivated by these advantageous attributes of GPEs, a new surface modification strategy to overcome the aforementioned limitations of inorganic material-based coatings is demonstrated. This is based on direct UV-assisted conformal coating of nanometer-thick poly(tris(2-(acryloyloxy)ethyl) phosphate) (PTAEP) GPE layers on an as-formed cathode.

The PTAEP bearing tri-functional vinyl groups [20] is employed as a coating material owing to the facile formation of crosslinked polymer matrix and excellent GPE performance (after being soaked with liquid electrolyte). Importantly, the phosphate groups of PTAEP are known to exhibit good chemical resistance and strong affinity for metal ions [16,17,21,22], which in turn could beneficially influence the interfacial stability between the PTAEP-coated cathode material and liquid electrolyte. As a cathode system, layer-structured $LiNi_{1/3}Co_{1/3}Mn_{1/3}O_2$ (NCM), one of the most widely used cathode materials in commercial lithium-ion batteries, is chosen.

The UV-irradiation, which has processing advantages such as short exposure time and no requirement for the use of a solvent [23–25], is exploited as a simple and scalable way to enable direct fabrication of conformal PTAEP nanocoating layers on NCM cathodes. Here, in order to effectively introduce the PTAEP coating layers on NCM surface without disrupting the preformed physical architecture (specifically, electronic networks and porous regions imparting ion-conductive channels) of the NCM cathode, UV-crosslinking reaction of TAEP monomers is carried out directly on as-formed NCM cathode, instead of applying to NCM powders.

Based on a comprehensive structural characterization of the PTAEP-coated NCM (hereinafter, referred to as “PTAEP-NCM”) cathode, beneficial effects of conformal PTAEP nanocoating layer (acting as an ion-conductive protective film that mitigates undesired interfacial side reactions between delithiated NCM and liquid electrolytes) on the cell performance and thermal stability of high-voltage (herein, 4.6 V) NCM cathode are scrutinized.

2. Experimental

A NCM cathode was prepared by coating a NMP-based slurry with a mixture of 90 wt% NCM (D_{50} = 10 um, BET surface area-= 0.294 $m^2\ g^{-1}$, Daejung EM), 5 wt% polyvinylidene fluoride (PVdF) binder, and 5 wt% carbon black on an aluminum current collector. Subsequently, the preformed NCM cathode was dipped into a coating solution (acetone was chosen as a solvent) containing 0.5 wt% TAEP monomer and 2-hydroxy-2-methyl-1-phenyl-1-propanon (HMPP, photo-initiator), where the HMPP concentration was fixed at 0.1 wt% of TAEP monomer content. The detailed synthesis and characterization of TAEP monomer were described in a previous publication [20]. The very low TAEP concentration of the coating solution is expected to allow facile infiltration of the coating solution into the preformed porous NCM cathode along its thickness direction. After evaporation of the solvent, the cathode was exposed to UV-irradiation (a Hg UV lamp [24,25] with an irradiation peak intensity of approximately 350 mW cm^{-2}) for 10 min, leading to the formation of UV-cured PTAEP coating layer on NCM surface. This stepwise fabrication procedure of the PTAEP-NCM cathode is schematically illustrated in Fig. 1(a).

The structural uniqueness of the PTAEP-NCM cathode was examined using a field emission scanning electron microscope (FE-SEM, Hitachi) equipped with an energy-dispersive spectrometer (EDS) and a transmission electron microscope (TEM, JEOL). The UV-crosslinking reaction of the PTAEP was analyzed with a FT-IR spectrometer (Excalibur). A unit cell (2032-type coin) was assembled by sandwiching a PE separator (thickness = 20 μm, Tonen) between a lithium metal anode and the abovementioned PTAEP-NCM cathode. The cell was then activated by being filled with a liquid electrolyte of 1 M $LiPF_6$ in EC/DMC = 1/1 v/v (Soulbrain). The charge/discharge behaviors of cells were evaluated using a battery test equipment (PNE Solution). The discharge capacities and C-rate capability were evaluated by varying discharge current densities (i.e., discharge C-rates) from 0.5 C (= 0.82 mA cm^{-2}) to 10.0 C at a constant charge current density of 0.5 C under a voltage range of 2.8–4.6 V. The cells were cycled at a constant charge/discharge current density of 1.0 C/1.0 C. The AC impedance of cells was measured using an impedance analyzer (VSP classic, Bio-Logic) over a frequency range of 10^{-3} to 10^{6} Hz. The exothermic reaction between the delithiated NCM and liquid electrolyte was examined by differential scanning calorimetry (DSC, DuPont) measurements [18,19].

3. Results and discussion

Fig. 2(a) shows the cross-sectional morphology of the PTAEP-NCM cathode, which reveals that a large area of the NCM surface is coated with the smooth and continuous PTAEP layer, although perfect surface coverage is not achieved. In addition, it is of note that the carbon black networks (offering electron-conductive networks) and the porous regions (to be filled with liquid electrolyte) are well preserved in the PATEP-NCM cathode. This demonstrates that the introduction of the PTAEP coating layer does not impair the preformed structural integrity of the NCM cathode.

This unusual structure of the PTAEP-NCM cathode was further examined by a TEM analysis. Fig. 2(b) shows that the NCM is well covered with the nanometer-thick PTAEP coating layer (thickness ~ 20 nm). The acrylate and phosphate groups [16,17,21,22] of the PTAEP may show strong affinity for NCM, thereby facilitating formation of the conformal PTAEP nanocoating layer. The EDS spectrum (Fig. 2(c)) presents the characteristic peak assigned to phosphor (P) of PTAEP, which is another evidence confirming the presence of the PTAEP coating layer on the NCM surface.

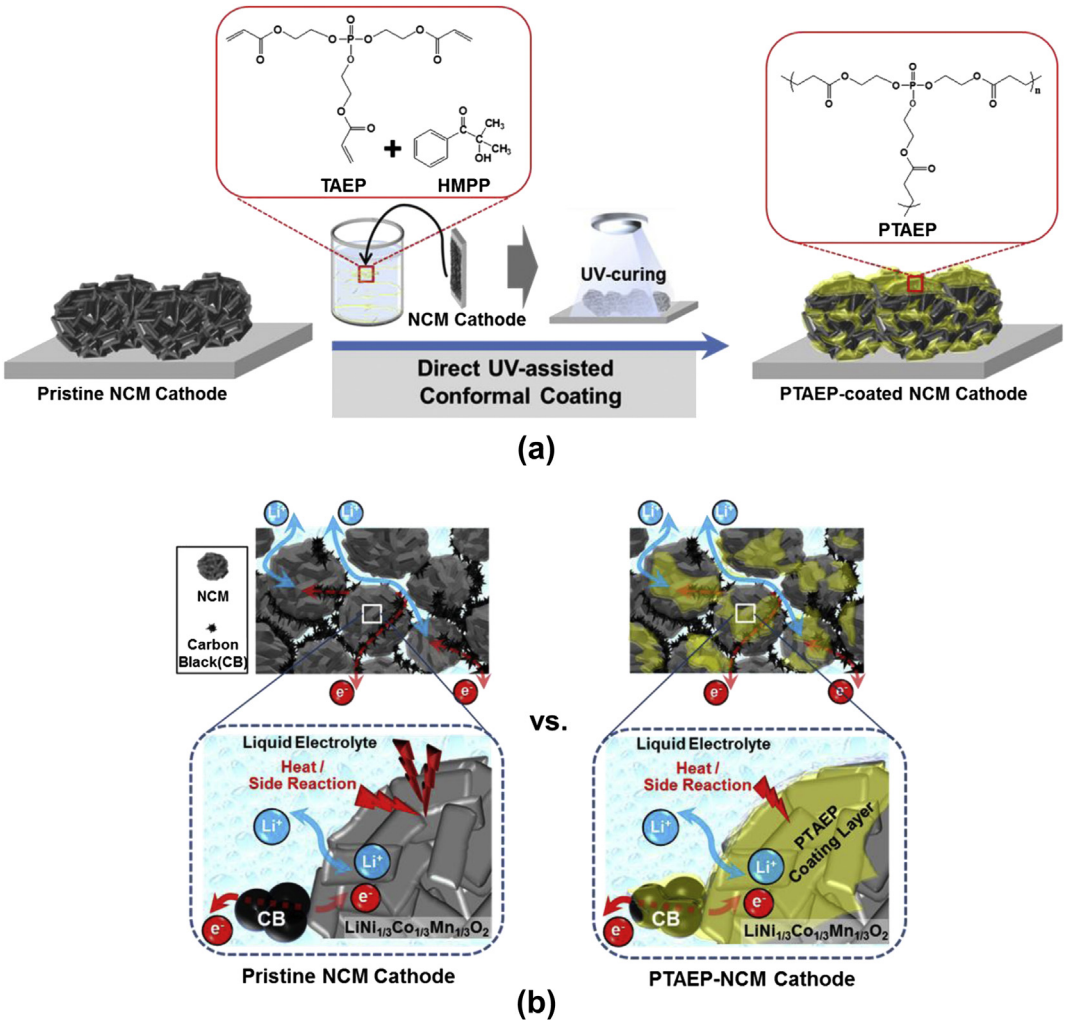

Fig. 1. (a) A schematic representation illustrating the stepwise fabrication procedure of PTAEP-NCM cathode, wherein chemical structure of PTAEP is depicted. (b) Schematic representations illustrating the structural uniqueness of conformal PTAEP nanocoating layer in the PTAEP-NCM cathode and its advantageous role as an ion-conductive protective film.

The UV-curing reaction of the PTAEP was elucidated by analyzing the FT-IR peaks ascribed to acrylic C=C bonds (1610–1625 cm^{-1} [24,25]) of TAEP monomers before/after the UV-irradiation. Unfortunately, due to the small amount of PTAEP coating layers, it was difficult to obtain appreciable FT-IR results directly from the PTAEP-NCM cathode. Therefore, for the FT-IR characterization, a PTAEP thin film (thickness ~ 50 μm) was additionally prepared by exploiting the same UV-irradiation procedure as that applied to the PTAEP-NCM cathode. Fig. 2(d) exhibits that the characteristic FT-IR peaks corresponding to C=C bonds of PTAEP disappear after the UV-irradiation, verifying the successful UV-curing reaction of the TAEP monomers. This is also confirmed by measuring the gel content of the PTAEP thin film. The gel content (i.e., insoluble polymer fraction after being subjected to solvent (dimethyl carbonate → acetone) extraction [24,25]) of the PTAEP film was found to be more than 99%. These results of FT-IR characterization and gel content, although indirect information of the UV-polymerization was provided, demonstrate that the UV-curing reaction used in this study is an effective way to form the crosslinked PTAEP coating layers.

Fig. 3(a) shows the effect of PTAEP coating layer on the discharge performance of cells charged to 4.6 V, where the discharge current densities were varied from 0.5 to 10.0 C at a constant charge current density of 0.5 C. The initial discharge capacities of the cells are found to be around 190 mAh g^{-1} at a discharge current density of 0.5 C. The voltage and discharge capacity of the cells gradually decrease with an increase of discharge current density, revealing the influence of ohmic polarization (i.e., IR drop [18,19]) on the cell performance. Intriguingly, due to the morphological advantages of the NCM particles (i.e., nanosized primary particle-aggregated spherical secondary particles [11–16]), the pristine NCM cathode delivers considerably high discharge capacities (~140 mAh g^{-1}) even at a high discharge current density of 10 C (the inset of Fig. 3(a)).

A notable finding is that the overall discharge capacities of the PTAEP-NCM cathode are almost comparable to those of the pristine NCM cathode over a wide range of discharge current densities, although the very slight deterioration in the discharge capacities and ohmic polarization (the inset of Fig. 3(a)) is observed in the PTAEP-NCM cathode. This indicates that the electronic networks and porous structure (to be filled with liquid electrolyte) of the PTAEP-NCM cathode are negligibly impaired and the additional ionic resistance possibly arising from the presence of the PTAEP coating layer may not be influential due to its nanometer-thick (~20 nm) surface coverage and facile ionic transport, although the PTAEP-NCM cathode shows the small increase in the AC

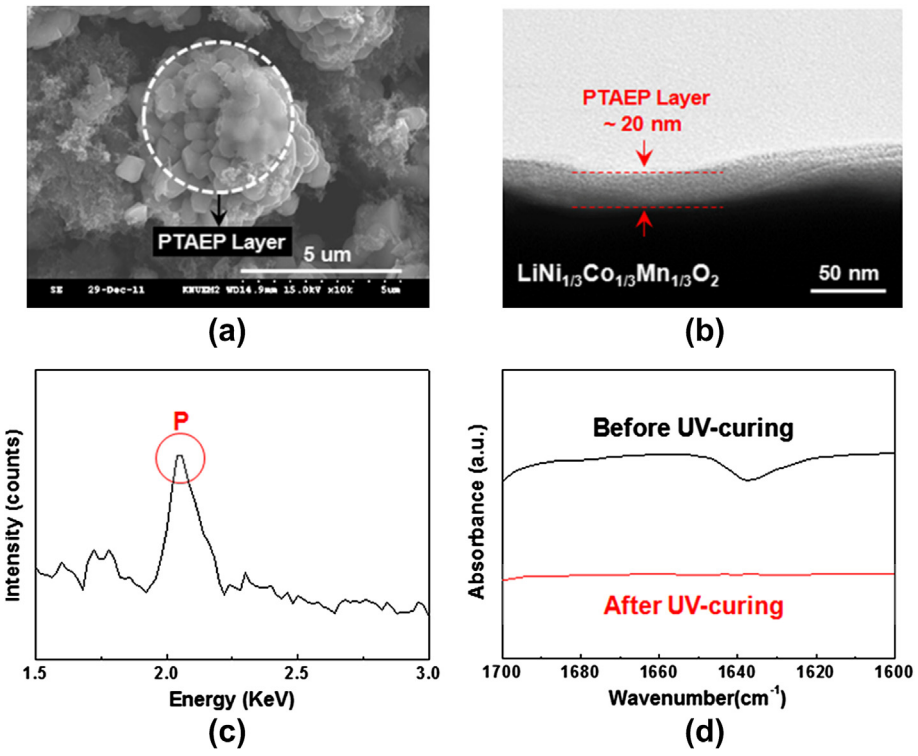

Fig. 2. Structural characterization of PTAEP-NCM cathode: (a) FE-SEM photograph; (b) TEM photograph; (c) EDS spectrum showing the characteristic peak assigned to phosphor (P) of PTAEP; (d) comparison of FT-IR peaks ascribed to acrylic C=C bonds (1610–1625 cm^{-1}) of TAEP monomers before/after the UV-irradiation.

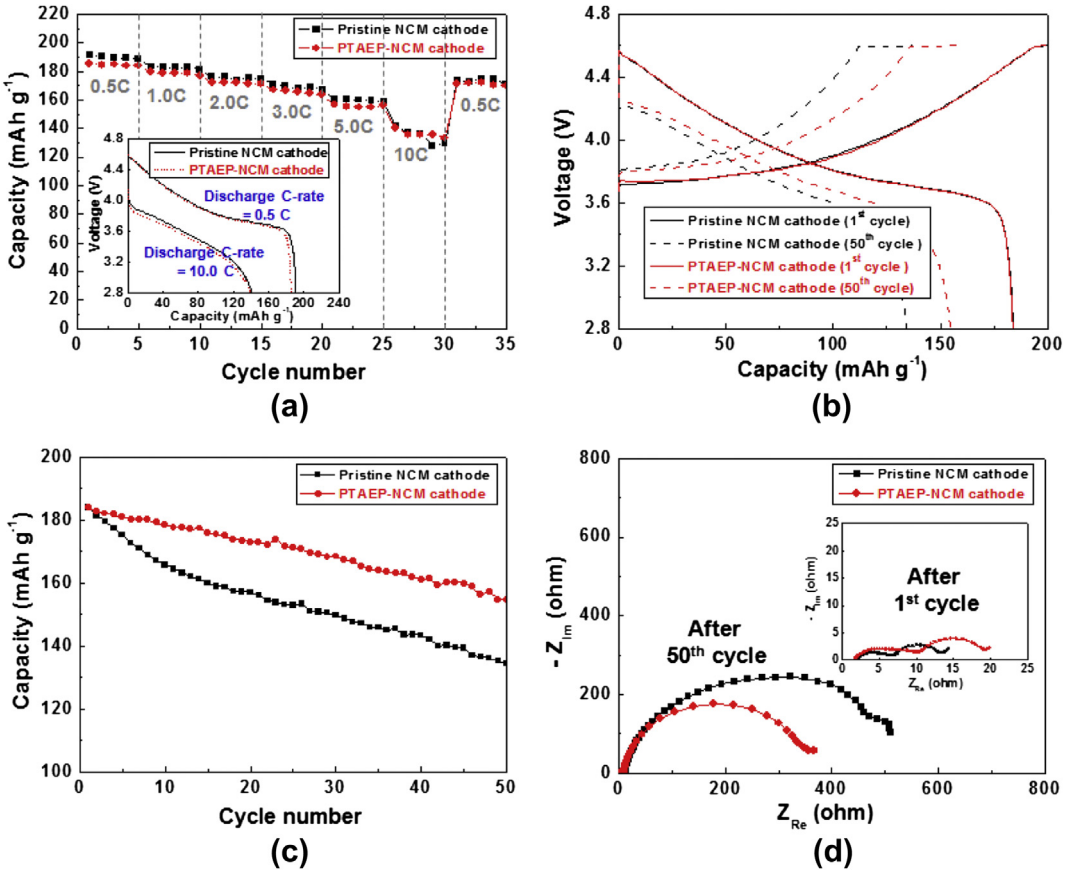

Fig. 3. 4.6 V cell performance of pristine NCM or PTAEP-NCM cathode: (a) discharge C-rate capability (an inset shows discharge profiles at a discharge current density of 0.5 C or 10.0 C); (b) charge/discharge profiles after 1st and 50th cycle; (c) cycling performance; (d) variation in AC impedance spectra (1st → 50th cycle) of cells.

impedance of cells (the inset of Fig. 3(d)). Here, a supplementary experiment for evaluating the ionic conductivity of PTAEP film swelled with the liquid electrolyte (1 M $LiPF_6$ in EC/DMC = 1/1 v/v) was carried out. The electrolyte-swollen PTAEP film was observed to deliver a high ionic conductivity of 0.32 mS cm^{-1} at room temperature. The unusual electronic/ionic transport phenomena in the PTAEP-NCM cathode, along with its structural uniqueness, are schematically illustrated in Fig. 1(b).

The effect of the PTAEP-NCM cathode on the high-voltage (4.6 V) cycling performance of cells was examined, wherein the cells were cycled under a constant charge/discharge current density (=1.0 C/1.0 C). The charge/discharge profiles of cells (Fig. 3(b)) show that the capacity loss and ohmic polarization during cycling are alleviated in the PTAEP-NCM cathode, as compared to those of the pristine NCM cathode. The capacity retention (as a function of cycle number) of the NCM cathodes is summarized in Fig. 3(c). As the cycle number is increased, the capacity fading of the PTAEP-NCM cathode is significantly mitigated, whereas the discharge capacity of the pristine NCM cathode continues to fall sharply. The capacity retention after the 50th cycle is found to be 73% for the pristine NCM cathode and 84% for the PTAEP-NCM cathode. This improvement in the high-voltage cycling performance of the PTAEP-NCM cathode, although the capacity fading does not yet reach satisfactory level, demonstrates that the PTAEP coating layer protects the NCM surface from attack of the violent liquid electrolyte, which consequently suppresses the harmful interfacial side reactions [11–15,21] between the NCM and liquid electrolyte. More fine-tuning of the PTAEP coating layer, which may include the optimization of its chemical structure and surface coverage, will contribute to further enhancing the high-voltage cycling performance. This will be one of our primary research interests in future studies.

In order to attain a better understanding of the influence of the PTAEP-NCM cathode on the cycling performance, the AC impedance spectra (after 1st and 50th cycle) of charged cells were analyzed. It has been known [12–16,26] that, from the analysis of possible equivalent circuit models of cells, the semicircle of impedance spectra at high frequency ranges represents the resistance of surface film on the electrode materials and the semicircle observed at medium-to-low frequency regions is ascribed to the charge transfer resistance between the electrode active materials and liquid electrolyte. Fig. 3(d) exhibits that the cell impedance of the pristine NCM cathode remarkably increases after the 50th cycle (Z_{Re} (50th cycle) − Z_{Re} (1st cycle) = $\Delta Z_{Re} \cong$ 500 ohm). This indicates that unwanted resistive layers could be continuously formed on the NCM surface during cycling, due to undesired interfacial side reactions between the charged NCM and liquid electrolyte. The resistive layer may hinder charge transfer via the interface between the NCM and liquid electrolyte, which would consequently give rise to the growth of cell impedance during cycling.

In comparison, the growth of cell impedance during cycling is retarded in the PTAEP-NCM cathode ($\Delta Z_{Re} \cong$ 340 ohm), which is also closely related with the alleviated ohmic polarization of the charge/discharge profiles after the 50th cycle (Fig. 3(b)). This demonstrates that the PTAEP coating layer effectively hampers direct exposure of charged NCM to the liquid electrolyte during the high-voltage cycling. Hence, the decomposition of liquid electrolyte on the NCM surface is highly suppressed, contributing to the good cycling performance. The advantageous role (as an ion-conductive protective film that suppresses unwanted interfacial side reactions) of the conformal PTAEP nanocoating layer is schematically illustrated in Fig. 1(b).

Fig. 4 depicts the DSC thermograms of the pristine NCM and PTAEP-NCM cathodes charged to 4.6 V. Previous studies [12–21] have reported that, in the DSC characterization, reduction of exothermic heat or shift of exothermic peak temperatures to higher

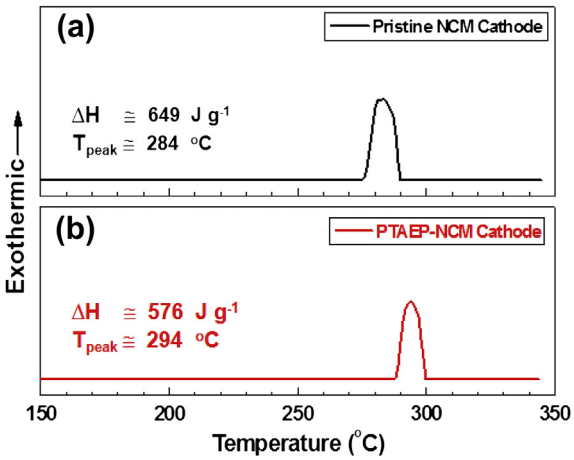

Fig. 4. DSC thermograms showing exothermic reaction between 4.6 V-charged NCM and liquid electrolyte: (a) pristine NCM cathode; (b) PTAEP-NCM cathode.

values accounts for thermally stabilized interface between electrode materials and liquid electrolyte. The pristine NCM cathode (Fig. 4(a)) yields relatively large exothermic heat ($\Delta H \cong$ 649 J g^{-1}) and low exothermic peak temperature ($T_{peak} \cong$ 284 °C), which is due to the vigorous exothermic reaction of the delithiated NCM with liquid electrolyte [12,16–21]. In comparison, for the PTAEP-NCM cathode (Fig. 4(b)), the exothermic heat is reduced ($\Delta H \cong$ 576 J g^{-1}) and T_{peak} shifts to a high temperature of 294 °C. This indicates that the PTAEP coating layer with high surface coverage effectively prevents the NCM from being directly exposed to the liquid electrolyte, which in turn alleviates the exothermic reaction between the delithiated NCM and liquid electrolyte. A schematic illustration conceptually explaining this improved thermal stability of the PTAEP-NCM cathode, as compared to the pristine NCM, is presented in Fig. 1(b).

4. Conclusion

In this study, the direct UV-assisted conformal coating of PTAEP layers on the as-formed NCM cathode was presented as a novel surface modification approach for high-voltage NCM. The salient features of the PTAEP coating layers were the nanometer-thick (~20 nm), highly-continuous surface coverage and no disruption of the preformed structural integrity (i.e., electronic networks and porous regions offering ion-conductive channels) of NCM cathode. Owing to this structural uniqueness, the PTAEP-NCM cathode substantially improved the 4.6 V cycling performance and suppressed the exothermic reaction between the delithiated NCM and liquid electrolyte, without impairing discharge C-rate capability. This demonstrated that the PTAEP nanocoating layer serves as a new ion-conductive protective film that effectively mitigates undesired interfacial side reactions, which are considered a formidable threat to electrochemical performance and thermal safety of high-voltage cells. We believe that the direct UV-assisted conformal coating strategy is highly versatile and thus can be readily applicable to other electrodes having a wide variety of electrochemical characteristics.

Acknowledgments

This research was supported by the MKE (The Ministry of Knowledge Economy), Korea, under the ITRC (Information Technology Research Center) support program (NIPA-2012-H0301-12-1009) supervised by the NIPA (National IT Industry Promotion Agency).

References

[1] G.J. Jeong, Y.U. Kim, H.S. Kim, Y.J. Kim, H.J. Sohn, Energy Environ. Sci. 4 (2011) 1986.
[2] P.G. Bruce, B. Scrosati, J.M. Tarascon, Angew. Chem. Int. Ed. 47 (2008) 2930.
[3] H. Li, Z. Wang, L. Chen, X. Huang, Adv. Mater. 21 (2009) 4593.
[4] C. Liu, F. Li, L.P. Ma, H.M. Cheng, Adv. Mater. 22 (2010) E28.
[5] F. Cheng, J. Liang, Z. Tao, J. Chen, Adv. Mater. 23 (2011) 1695.
[6] J.B. Goodenough, Y.S. Kim, Chem. Mater. 22 (2010) 587.
[7] B.L. Ellis, K.T. Lee, L.F. Nazar, Chem. Mater. 22 (2010) 691.
[8] Y.K. Sun, J.M. Han, S.T. Myung, S.W. Lee, K. Amine, Electrochem. Commun. 8 (2006) 821.
[9] Z. Yang, W. Yang, D.G. Evans, G. Li, Y. Zhao, Electrochem. Commun. 10 (2008) 1136.
[10] S.S. Hwang, C.G. Cho, K.S. Park, Electrochem. Commun. 13 (2011) 279.
[11] S.T. Myung, K. Izumi, S. Komaba, Y.K. Sun, H. Yashiro, N. Kumagai, Chem. Mater. 17 (2005) 3695.
[12] Y. Huang, J. Chen, F. Cheng, W. Wan, W. Liu, H. Zhou, X. Zhang, J. Power Sources 195 (2010) 8267.
[13] S.K. Hu, G.H. Cheng, M.Y. Cheng, B.J. Hwang, R. Santhanam, J. Power Sources 188 (2009) 564.
[14] R. Guo, P. Shi, X. Cheng, L. Sun, Electrochim. Acta 54 (2009) 5796.
[15] K.S. Lee, S.T. Myung, D.W. Kim, Y.K. Sun, J. Power Sources 196 (2011) 6974.
[16] D.J. Lee, B. Scrosati, Y.K. Sun, J. Power Sources 196 (2011) 7742.
[17] J.P. Cho, Y.W. Kim, B.S. Kim, J.G. Lee, B.W. Park, Angew. Chem. Int. Ed. 42 (2003) 1618.
[18] J.H. Park, J.S. Kim, E.G. Shim, S.Y. Lee, Electrochem. Commun. 12 (2010) 1099.
[19] J.H. Cho, J.H. Park, H.K. Song, S.Y. Lee, Energy Environ. Sci. 5 (2012) 7124.
[20] J.A. Choi, Y.K. Kang, H.J. Shim, D.W. Kim, H.K. Song, D.W. Kim, J. Power Sources 189 (2009) 809.
[21] H.G. Song, J.Y. Kim, K.T. Kim, Y.J. Park, J. Power Sources 196 (2011) 6847.
[22] G. Li, Z. Yang, W. Yang, J. Power Sources 183 (2008) 741.
[23] C. Gerbaldi, J.R. Nair, G. Meligrana, R. Bongiovanni, S. Bodoardo, N. Penazzi, Electrochim. Acta 55 (2010) 1460.
[24] E.H. Kil, H.J. Ha, S.Y. Lee, Macromol. Chem. Phys. 212 (2011) 2217.
[25] H.J. Ha, J.Y. Kim, S.Y. Lee, Energy Environ. Sci. 5 (2012) 6491.
[26] J. Liu, A. Manthiram, J. Phys. Chem. C 113 (2009) 15073.